Polymer Testing 81 (2020) 106164

Contents lists available at ScienceDirect

Polymer Testing

journal homepage: http://www.elsevier.com/locate/polytest

Development of a simple setup for temperature dependent mass spectrometric measurements for the investigation of outgassing effects in polymeric materials for solar application

Andreas Piekarczyk [a,b,*], Ulrike Heitmann [a], Karl-Anders Weiß [a], Michael Köhl [a], Ilko Bald [c]

[a] Fraunhofer Institute for Solar Energy Systems ISE, Freiburg, Germany
[b] Faculty of Environment and Natural Resources, University of Freiburg, Freiburg, Germany
[c] Faculty of Science, University of Potsdam, Potsdam, Germany

A B S T R A C T

A simple experimental setup for temperature dependent mass spectrometric measurements has been constructed. It consists of a heated sample chamber and a mass spectrometer and allows for measurements under inert gas and ambient air. Based on initial measurements on two extruded polystyrene (XPS) samples a methodology for the data analysis has been developed. With this methodology the outgassing temperature of volatile compounds, which were used as blowing agents, has been identified. Furthermore, the composition of the blowing agents has been analyzed by temperature dependent mass spectra. The results indicate the use of ambient air in one material and a mixture of the banned blowing agents R142b and R22, both hydrochlorofluorocarbons (HCFC), in the other material. The here described methodology provides an easy to use approach to identify such compounds, for example as part of environmental or quality control.

1. Introduction

Polymeric materials are frequently used in solar energy systems and have been optimized for such applications over the years. The use of polymers for major components of solar thermal systems has been investigated with the focus on the aging behavior of these materials [1–4]. In fully polymeric solar thermal collectors many different polymers are used in the same collector [5–9]. During operation the polymeric materials are repeatedly and for a long period of time exposed to temperatures above 120 °C. Since normally the service life time of solar thermal systems is expected to be at least 20 years the materials developed for such applications are individually tested for aging effects by standard testing methods. However, in a closed volume, such as the inside of a solar thermal collector, possible outgassing from the materials [10,11] and a possible interaction of the outgassing products with all other components of the solar thermal system may affect the long term stability and need to be considered. Volatile compounds originating from a polymer can be additives with small molecular mass, such as certain plasticizers, or fragments of additives with larger molecular mass or of the polymer matrix. The loss of volatile plasticizers will lead to changes in the mechanical properties of the polymer. The detection of volatile fragments originating from other additives or the polymer matrix can be an indicator for the degradation of the polymer itself, for example due to thermal decomposition or oxidation. In the closed volume such volatile compounds can accumulate and possibly migrate into the polymeric materials of other components of the collector, acting as plasticizers or initiating new degradation effects, and changing the material properties of the given component. In order to evaluate such possible material interactions through outgassing processes the outgassing behavior of all individual polymeric materials used needs to be studied for the temperature range of the operation conditions.

Comparable methods such as thermal volatilization analysis (TVA), evolved gas analysis (EGA) [12] or evolved gas detection (EGD) have been described earlier [13] and combine often thermogravimetric analysis (TG) with mass spectrometric measurements (MS) [14,15]. Thus, many methods require a high technical effort and have shown only limited applicability to complex mixtures. This is because polymers contain only small amounts of volatile compounds and increased temperatures lead to decomposition of the polymer matrix [16]. Through significant technological progress in the last decades, mass spectrometers have become more compact and less expensive making them more suitable for routine analytical tasks [14].

The here described experimental setup has been developed to measure the change of the gas phase composition above a polymer sample throughout heating as a function of the temperature. The aim is to develop a methodology allowing the attribution of all compounds of the gas phase to their formation processes at elevated temperatures, which can be observed at operating conditions of polymeric solar thermal collectors. In order to make the experimental setup presented here a

* Corresponding author. Fraunhofer Institute for Solar Energy Systems ISE, Freiburg, Germany.
E-mail address: andreas.piekarczyk@mail.nature.uni-freiburg.de (A. Piekarczyk).

https://doi.org/10.1016/j.polymertesting.2019.106164
Received 2 July 2019; Received in revised form 9 October 2019; Accepted 14 October 2019
Available online 14 October 2019
0142-9418/© 2019 Elsevier Ltd. All rights reserved.

Nomenclature

amu	atom mass unit
EGA	evolved gas analysis
EGD	evolved gas detection
HCFC	hydrochlorofluorocarbon
I	signal intensity as ion current in mA
m/z	mass to charge ratio
MS	mass spectrometry
R142b	1-Chloro-1,1-difluoroethane
R22	chlorodifluoromethane
T	temperature in °C
TG	thermogravimetric analysis
TVA	thermal volatilization analysis
U	unified atomic mass unit
X	any given mass to charge ratio
XPS	extruded polystyrene

useful screening tool for various applications, it should allow for a broad variation of measurement parameters like the variation of the gas phase composition and pressure, for example to study the impact of the oxygen concentration on the thermal oxidation of the materials. Further it requires a minimal effort for sample preparation and allows different material shapes and sizes making the testing of wrought products possible. Another requirement is a simple data analysis allowing for screening of material variations for the outgassing of volatile organic compounds. The setup has been tested on two materials presumed suitable for polymeric solar thermal collectors.

2. Experimental section

2.1. Experimental setup

The experimental measurement setup consists of two basic components; a heated test chamber and a mass spectrometer. The used chamber is an in-house design made of modified stainless-steel flanges for ultra-high vacuum applications and equipped with a pressure sensor (APR 262 Active Piezo Transmitter, Pfeiffer Vacuum, Germany).

Right: Sample chamber with electric heater, gas installation and temperature sensor.

The chamber is heated with an electric heating plate allowing a uniform heat distribution inside the chamber. The temperature is monitored with an integrated thermocouple temperature sensor. Three fittings connect the test chamber to a vacuum line, purge gas line and the mass spectrometer. The mass spectrometer is connected through a heated stainless-steel capillary to the test chamber (Fig. 1). The diameter of the capillary is 130 µm and leads to a pressure gradient of approximately 1 bar inside the test chamber and 5×10^{-8} mbar inside the mass spectrometer.

A quadrupole mass spectrometer (Omni Star GSD 320 O1, Pfeiffer Vacuum, Germany) with a mass range of 0–100 a.m. was used for detecting the composition of the gas atmosphere. Ions were detected with the built-in secondary electron multiplier (SEM) detector. Signals were processed with the instrument's Software Quadera® (v. 4.40). For the detected ions the SEM signal is recorded as ion current (I) for each mass to charge ratio (m/z).

2.2. Materials

Two different samples of extruded polystyrene (XPS) were used as model systems for outgassing measurements. The two samples are anonymized and are referred to as XPS-A and XPS-B.

2.3. Procedure and data processing

The polymer samples are placed on a thin aluminum foil and inserted into the heating chamber. The chamber is sealed by a copper gasket. To reduce the oxidation of the samples the chamber can be evacuated and flushed with inert gas prior to measurements. As air is commonly used as blowing agent in XPS the use of a different inert gas than nitrogen as main component increases the sensitivity of the measurement. Therefore, the atmosphere inside the test chamber has been mostly replaced with helium leaving only traces of atmospheric gases for measurements of XPS samples. During this purge process the gas composition can also be monitored.

While the sample chamber is heated up from room temperature to 250 °C the gas composition inside the sample chamber is monitored by mass spectrometry. For measurements under ambient air atmosphere the procedure is the same, except no purging is required prior to the measurement. The measurement is initiated with the beginning of the heating process. The temperature inside the chamber is increased to 250 °C following a linear heating curve (see Table 1). The temperature is recorded in intervals of 2 min. Mass spectra are recorded in fixed time intervals defined for each measurement. Based on the heating curve the acquired time dependent spectra are transformed into temperature dependent spectra. For this purpose, the heating curve is interpolated with the same amount of data points as spectra data points available and

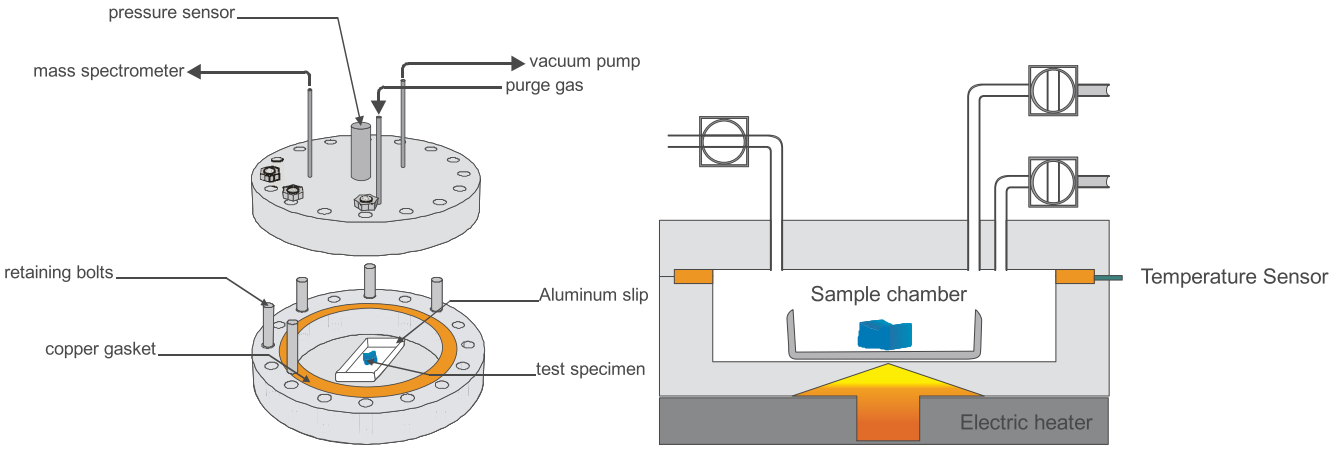

Fig. 1. Left: Test chamber made of stainless-steel flanges for ultra-high vacuum application with copper gaskets. The test specimen is inserted into the test chamber and the chamber is sealed to preserve a contamination of the atmosphere with ambient air. Installed connectors to a vacuum pump and purge gas allow measurements under inert gas atmosphere or ambient air.

Table 1
Overview of measured samples with detailed parameters for heating rate and pressure inside the test chamber at the beginning of the measurement. In the following the measurements at 700 mbar pressure will be referred to as reduced pressure.

Pressure	XPS-A	XPS-B
1000 mbar	r = 2.7 K/min	r = 2.7 K/min
700 mbar	r = 2.5 K/min	r = 2.5 K/min

the time of measurement is replaced by the temperature during the given measurement. The temperature dependent data are then analyzed by changes of *m/z* over the temperature or as mass spectra at individual temperatures. The contour plot hereby provides a graphical overview of *m/z* signals. In the following all dominant *m/z* signals are analyzed as a function of temperature.

The signal intensity in the described setup depends on the mass flow through the capillary, which depends on the pressure gradient between the test chamber and the mass spectrometer. With increasing pressure inside the test chamber the signal intensity is increasing. To compensate for the pressure increase as a result of the heating of the test chamber, the signal of the inert main component (nitrogen gas or helium) is used to normalize all other signals with respect to the inert gas.

3. Results

3.1. Measurement of the empty chamber

The empty chamber was measured according to the appropriate procedure with ambient air and helium as inert gas, respectively, in order to determine the background signals resulting from the chamber and to check for contaminations. The chamber was heated with a rate of 2.5 K/min and the composition of the gas phase monitored over time. In a second step the recorded time-dependent mass spectra were transferred into temperature dependent mass spectra. For the identification of relevant ion signals a 2D plot (analogous to Fig. 5) was used. For the analysis of the temperature dependence of the signal intensity the selected ion signals were plotted over temperature (Fig. 2). The dominant signals recorded for the empty chamber are listed in Table 2 and have to be considered as the signal background of the chamber. They are divided into five groups according to their temperature dependence. Most of these signals, among which *m/z* 28 and *m/z* 32 are the most dominant ones, can be attributed to atmospheric gases. Signals of group 1 have their origin in residues of humidity inside the test chamber. Singly and doubly ionized molecular oxygen is the primary source of the signals in group 2. The signals in group 3 are attributed to the inert components of the atmosphere inside the test chamber. In all measurements the presence of argon and nitrogen with both $^{28}N_2$ and $^{29}N_2$ can be observed. Helium is only detected when used as inert gas for the measurement and then the other signals are normalized to the helium signal.

Table 2
Groups of dominant signals (Group 1–4) resulting from the ambient air inside the chamber or residual air after purging with inert gas. Group 5 contains signals which can not be attributed to atmospheric gases and have their origin in organic contaminants inside the test chamber. *Signal with *m/z* 4 for helium is only found in measurements under helium atmosphere.

	Signals with *m/z*					Origin
Group 1	18	17	1			H_2O
Group 2	32	16				O_2; H_2O
Group 3	28	14	29	40	4	$^{28}N_2$;$^{29}N_2$; Ar; He*
Group 4	44	12	22			CO_2
Group 5	45	56	51			Unidentified compounds

Signals of group 4 can be assigned to carbon dioxide, both as atmospheric component and as product of oxidation processes. All other signals are attributed to group 5. The intensity increase of other signals with temperature is different from those of groups 1–4 and indicates the presence of residues inside the chamber.

In order to compensate for the signal increase (see Fig. 2) as result of the pressure increase inside the test chamber, data required normalization (Fig. 3). For the normalization different approaches (Equation (2)-Equation (4)) for the inert main component were tested and validated (Fig. 4). The use of nitrogen gas as an internal standard is also promising since the composition of atmospheric air can be considered constant for this application. The simplest approach for the normalization of an ion signal ($I_{m/z\ x}(T)$) at a temperature (T) of a given mass-to-charge-ratio (x) is by dividing it by the ion signal of the main inert component (i) at the same temperature (Equation (1)).

$$I_{m/z\ x;\ nor}(T) = \frac{I_{m/z\ x}(T)}{I_{m/z\ i}(T)} \quad (1)$$

This is possible for measurements under helium atmosphere, since no interaction of helium with other components has to be considered. The raw data can be directly normalized using the helium signal with *m/z* 4. The direct comparison of the signal intensity ratios for individual measurements however is not possible, because of small differences in the measurement conditions, such as different amounts of residual atmospheric gases after purging. The recording of a test chamber background for subtraction turned out to be an invalid procedure to improve the data analysis.

For the normalization of data of measurements under air atmosphere a normalization according to Equation (1) is not possible. Fig. 2 indicates oxidation processes of organic residues during the heating, as a signal increase for *m/z* 44 (CO_2) is observed and coincides with the decrease of signal intensity of *m/z* 32 (O_2). Thus also the formation of carbon monoxide (CO) during the heating process can not be ruled out. The ion signal of CO with *m/z* 28 coincides with the ion signal of $^{28}N_2$. Therefore Equation (2) is not applicable for the normalization of measurements under atmospheric air.

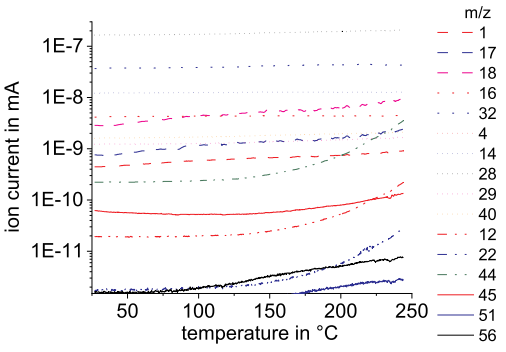

Fig. 2. Raw data recorded for the heating of the contaminated empty test chamber. Signals are listed as ion current.

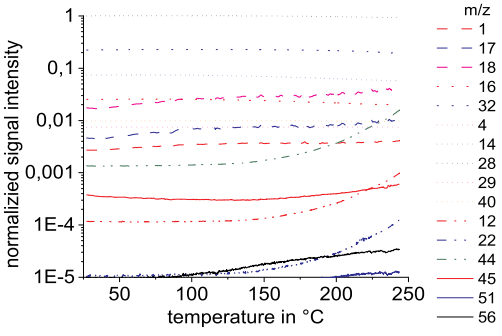

Fig. 3. Data normalized to the signal of $^{29}N_2$ using Equation (4).

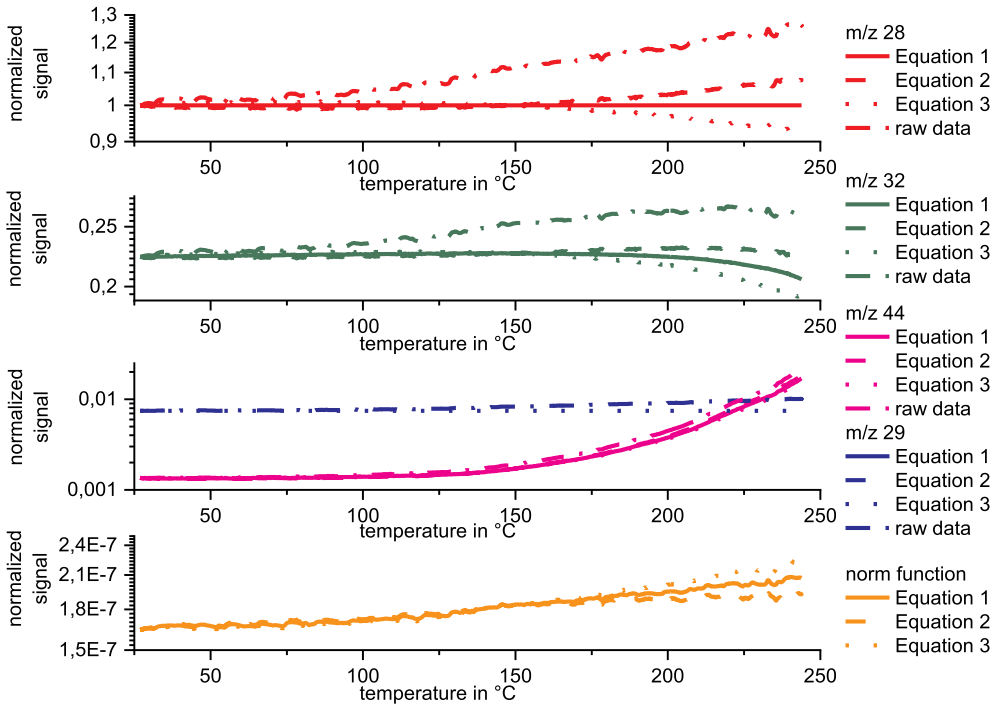

Fig. 4. Comparison of the different approaches for the normalization of the data and the resulting signal progressions. For comparison with the normalized data the signals for the raw data were scaled using the factor $I_{m/z\ 28}\ (T_0)$.

$$\boldsymbol{I}_{m/z\ x;\ nor}(\boldsymbol{T}) = \frac{\boldsymbol{I}_{m/z\ x}(\boldsymbol{T})}{\boldsymbol{I}_{m/z\ 28}\ (\boldsymbol{T})} \tag{2}$$

$$\boldsymbol{I}_{m/z\ x;\ nor}(\boldsymbol{T}) = \frac{\boldsymbol{I}_{m/z\ x}(\boldsymbol{T})}{\boldsymbol{I}_{m/z\ 28}\ (\boldsymbol{T})^2} \cdot \frac{\boldsymbol{I}_{m/z\ 29}\ (\boldsymbol{T}) \cdot \boldsymbol{I}_{m/z\ 28}\ (\boldsymbol{T}_0)}{\boldsymbol{I}_{m/z\ 29}\ (\boldsymbol{T}_0)} \tag{3}$$

$$\mathbf{I}_{\mathbf{m/z\ x;\ nor}}(\mathbf{T}) = \frac{\mathbf{I}_{\mathbf{m/z\ x}}(\mathbf{T})}{\mathbf{I}_{\mathbf{m/z\ 29}}\ (\mathbf{T})} \cdot \frac{\mathbf{I}_{\mathbf{m/z\ 29}}\ (\mathbf{T}_0)}{\mathbf{I}_{\mathbf{m/z\ 28}}\ (\mathbf{T}_0)} \tag{4}$$

Equation (3) is based on Equation (2) and has an additional correction term $((I_{m/z\ 29}\ (T))/\ (I_{m/z\ 28}\ (T)))$ using the isotopic ratio of the two isotopes $^{28}N_2$ and $^{29}N_2$ and an additional normalization term containing the ratio of both isotopes at T_0. By taking the ratio of these two isotopes into account the impact of overlapping signals of $^{28}N_2$ and ^{28}CO should be reduced to 1%. Using Equation (3) to normalize the data an increase of the signal intensity for *m/z* 32 over the heating process can be observed. Under given operational conditions this can only be explained by insufficient compensation of the pressure increase inside the test chamber.

Equation (4) is based on Equation (2) but uses only the signal intensity of *m/z* at the beginning of the measurement for normalization and a correction term containing only the signal at *m/z* 29 for compensating the pressure increase during the heating of the chamber. Using Equation (4) the observed signal progression is plausible and the observed decrease of the signal *m/z* 29 can be explained by the decreasing density of the atmosphere inside the test chamber through the measurement processes.

Fig. 3 shows only three signals of group 5 at m/z 45, 51, and 56, in the selected range of 1 and $1{\cdot}10^{-5}$ for normalized signals. This range is considered sufficient for this analysis as, for comparison, the normalized signal intensity of carbon dioxide with *m/z* 44 at the beginning of the illustrated measurement is $1{,}36{\cdot}10^{-5}$, which resembles the atmospheric concentration of 380 ppm. The three aforementioned signals (*m/z* 45, 51, and 56) indicate the presence of organic residues inside the empty test chamber which need to be considered when analyzing similar processes for sample materials.

3.2. Measurements of extruded polystyrene in inert atmosphere

Temperature dependent mass spectra have been recorded for XPS samples under an inert gas atmosphere at a pressure 1000 mbar (Fig. 5) and with a reduced pressure of 700 mbar (not illustrated). The contour plots in Fig. 5 provide a first indication of different thermal behavior of the two XPS materials XPS-A and XPS-B. An increase of signal intensity at several $m/z > 40$ at temperatures around 100 °C can be observed for samples of XPS-B, while most of these signals are not present for XPS-A. At this stage of the data analysis the two materials can be qualitatively evaluated with respect to the release of volatile compounds up to temperatures of 250 °C. It is evident that not all atmospheric gases were removed from the test chamber by the purge process. For semi-quantitative assessments the recorded data is processed further.

For further analysis the data was processed according to the procedure described in chapter 3.2 and normalized to the signal of helium with *m/z* 4. The intensity range for the further analysis of signals was selected analogously to chapter 4.1 to a normalized signal intensity between 1 and $1{\cdot}10^{-5}$. The dominant ion signals of all spectra were selected based on this range (Fig. 6 and Fig. 7). The intensities of the signals attributed to the groups 1–4 differ in the content of atmospheric gases relative to helium as main inert component. This ratio depends on the mass flow, the duration and the pressure during purging and the measurement and has shown to be difficult to maintain constant for the individual measurements. Both samples show a similar increase of signal intensity at temperatures above 80 °C. At this temperature a strong increase in intensity of most signals is observed. With regards to the melting temperature of the analyzed polymer it can be assumed that the blowing agent is evolving from the softening sample material. For sample XPS-A the increase occurs in a limited temperature range (80–90 °C) and only atmospheric gases are released. For sample XPS-B the increase in intensity is observed for a much wider temperature range. The signals, which show the highest increase in intensity, cannot be attributed to atmospheric gases. Among these the signals with *m/z* 65, 45 and 85 are the most dominant ones. Both samples show an increasing intensity for signals with *m/z* 51 and 78 with increasing temperature which are not found for the empty chamber. Both *m/z* 51

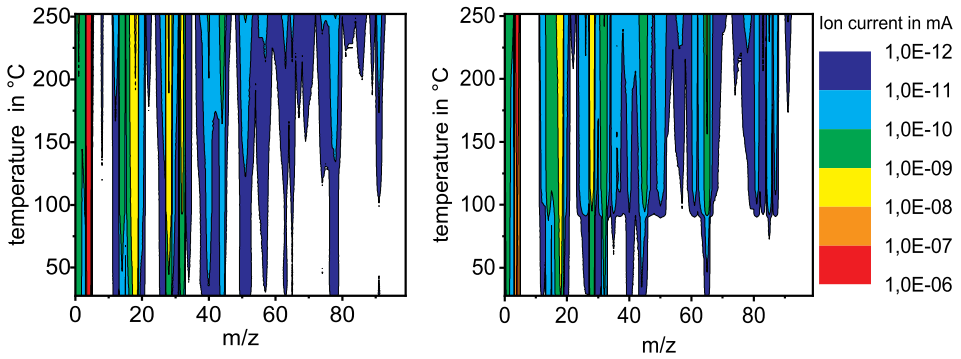

Fig. 5. Temperature dependent mass spectra for XPS-A (left) and XPS-B (right). Clearly visible is an increase of signal intensity in the temperature range of 80–100 °C for all *m/z* for both materials. This corresponds to the softening temperature of the material. XPS-B shows a more complex signal pattern for $m/z > 40$ indicating the use of a different blowing agent.

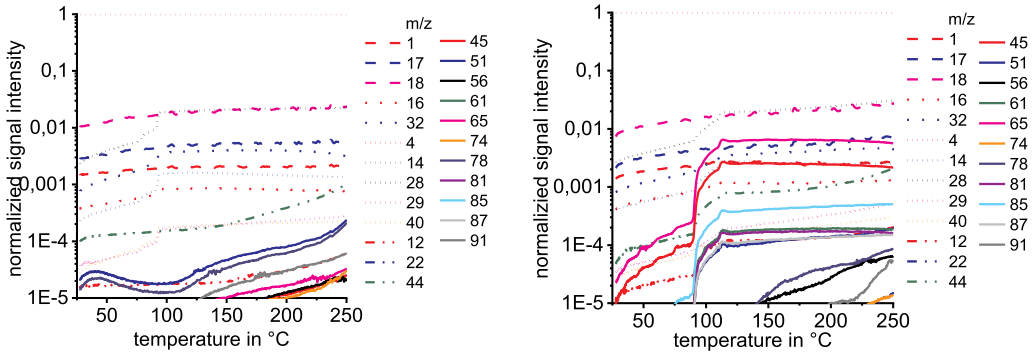

Fig. 6. Comparison of temperature dependent mass spectra of XPS-A (left) and XPS-B (right). Clearly visible is an increase of signal intensity in the temperature range of 80–100 °C for all *m/z* for both materials. This corresponds to the softening temperature of the material. XPS-B shows a more complex signal pattern in the range $m/z > 40$ indicating the use of a different blowing agent.

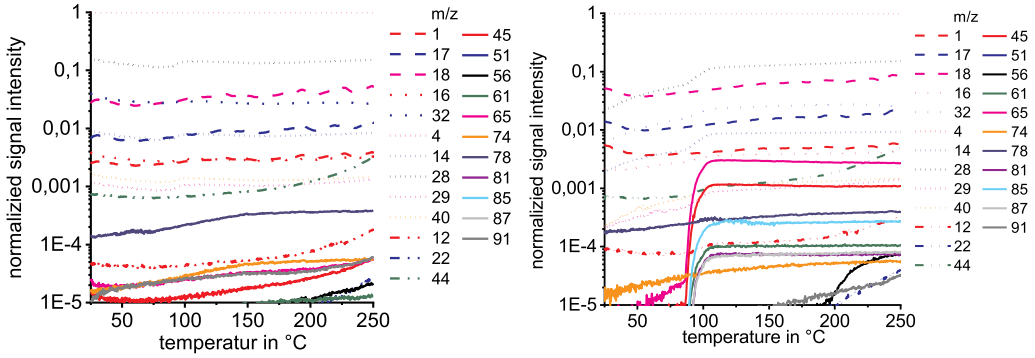

Fig. 7. Comparison of temperature dependent mass spectra of XPS-A (left) and XPS-B (right) measured under reduced pressure.

($C_4H_3^+$) and *m/z* 78 ($C_6H_6^+$) are major fragments of styrene [17], the monomer of XPS (Fig. 8 and Fig. 9). The signal *m/z* 91 is also a possible fragment formed from styrene oxide.

In all measurements an increase of *m/z* 44 with temperature is observed and can be attributed to oxidation processes of organic compounds inside the chamber. Since this is also observed for the empty chamber (see 4.1) it cannot be conclusively ruled out that it may also result from contaminations inside the chamber. However, it is safe to assume that the total signal intensity must be the result from both residues inside the chamber and oxidation products of the sample material. For the measurement under reduced pressure no such sudden increase around the softening temperature can be observed for the XPS-A samples (see Fig. 7 left). It can be assumed that a large amount of blowing agent was already released during the purge process at reduced pressure. While the same effect concerning atmospheric gases (group 1–4) is observed for the XPS-B samples which have been degassed during purging, a strong increase of signals of group 5 can be observed. This indicates that for XPS-B other gasses or a combination of air and additives have been used as blowing agent. Among the possible origins for the signal *m/z* 65 fragments of the type $C_2H_3F_2$ are possible according to the NIST database [17]. The use of R142b with the chemical formula $C_2H_3ClF_2$ can be considered as possible source for the *m/z* 65 and *m/z* 81 signals which would correspond to the fragment C_2H_3ClF.

Based on the possible use of HCFC as blowing agent the signals *m/z* 85 and 87 solely found for XPS-B can be attributed to the blowing agent R22 with the chemical formula $HCClF_2$ [18]. While the average molecular mass is 86.47 u there is no signal with *m/z* 86 observed in the respective mass spectra. However, chlorine has two stable isotopes ^{35}Cl

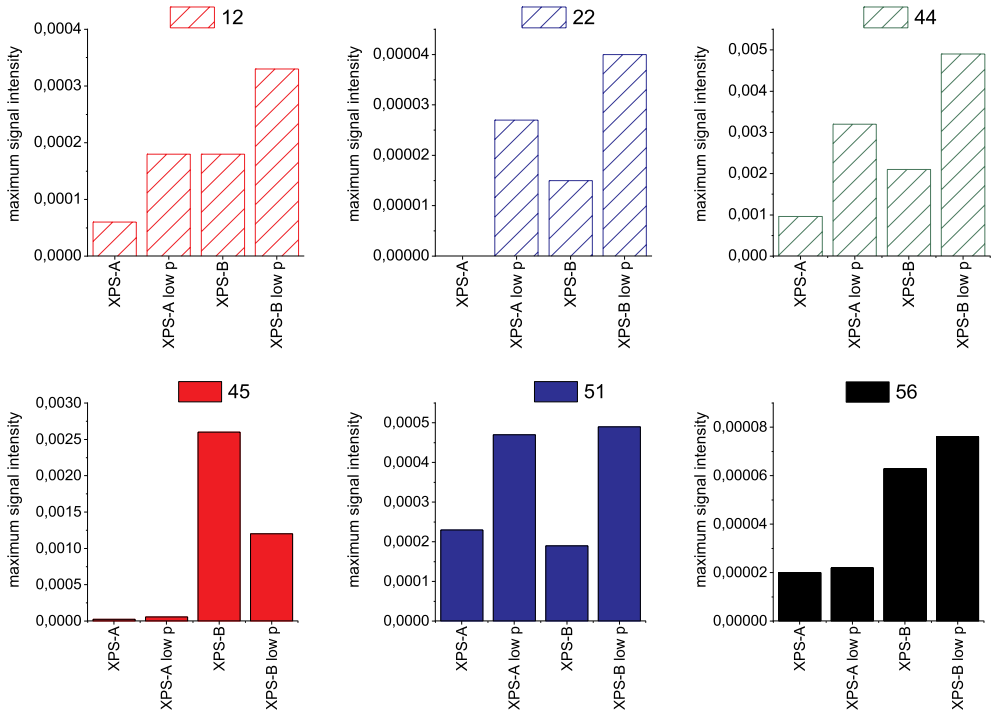

Fig. 8. Dominant signals at different *m/z* for the individual measurements sorted to signal groups with similar temperature dependency and allocation to signal origin. Intensity refers to the highest normalized signal intensity of the given *m/z* throughout the measurements. Signals with *m/z* 45, 51 and 56 are also found in the empty chamber.

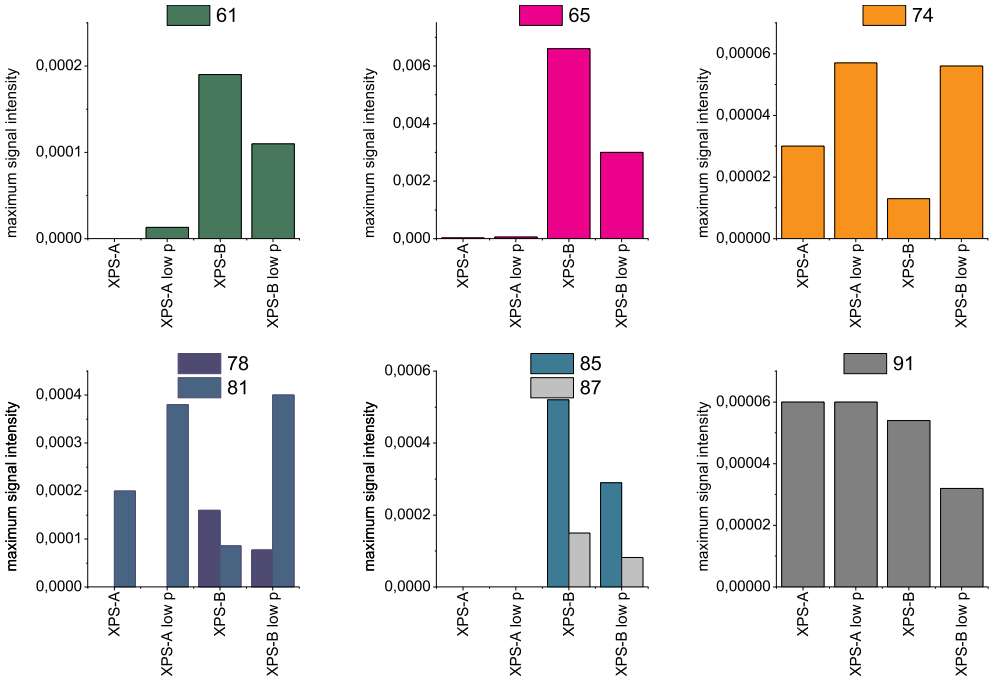

Fig. 9. Dominant signals at different *m/z* for the individual measurements sorted to signal groups with similar temperature dependency and allocation to signal origin. Intensity refers to the highest normalized signal intensity of the given *m/z* throughout the measurements. The signals with *m/z* 65, 85 and 87 occur only in measurements of XPS-B. The signals *m/z* 85 and 87 can be attributed to the blowing agent R22 with an average molecular mass of 86.47 u. The intensity ratio of the signals *m/z* 85 and 87 resembles the isotopic ratio of the two chlorine isotopes ^{35}Cl and ^{37}Cl.

and ^{37}Cl with a fixed ratio of 76/24 leading to two molecular species with 85 u and 87 u with the same ratio. The intensity ratio of the signals *m/z* 85 and 87 matches the isotopic distribution of chlorine in the compound $CHC^{35}ClF_2$ and $CH^{37}ClF_2$ with 77.6/22.3 extremely well and validates the assumption that the detected signals originate from the compound R22. Hence, it can be stated that the blowing agents R22 and R142b are used for XPS-B. The signals with *m/z* 61 and 74 cannot be identified without further knowledge of the materials' compositions. All relevant signals and the respective source they have been attributed to are listed in Table 3.

4. Discussion

Several measurement variations have been performed in order to evaluate the influence of the individual parameters on the obtained data. It has become evident that a more detailed analysis of oxidation

Table 3
Attribution to different sources of individual signals from group 5 found for XPS-A and XPS-B. Signals marked with * are also found in the chamber background and can therefore not be conclusively attributed to the samples.

Signals at *m/z*	XPS-A	XPS-B	Attributed to	Molecular formula
12	✓	✓	Oxidation	$^{12}C^+$
22	–	✓	Oxidation	CO_2^{2+}
44	✓	✓	Oxidation	CO_2^+
45*	✓	✓	Possible contamination	$C_2H_5O^+$
51*	✓	✓	Monomer	$C_4H_3^+$
56*	✓	✓	Possible contamination	$C_3H_4O^+$
61	✓	✓	Unknown origin	Unknown
65	✓	✓	Blowing agent R142b	$CF_2CH_3^+$
74	✓	✓	Unknown origin	Unknown
78	✓	✓	Monomer	$C_6H_6^+$
81	–	✓	Blowing agent R142b	$^{35}ClCFCH_3^+$
85	–	✓	Blowing agent R22	$^{35}ClCF_2^+$
87	–	✓	Blowing agent R22	$^{37}ClCF_2^+$
91	✓	✓	Monomer	$C_7H_7^+$

and outgassing processes requires normalization of the raw data in order to compensate for the increase of the signal intensity with the temperature and the pressure increase inside the test chamber. The proposed approach to normalize the raw data using the main inert component in the gas phase of the test chamber has been applied for atmospheric air and after a purge process for a helium/air mixture. It has been found that this procedure is not directly applicable to air, because the possible formation of carbon monoxide may interfere with the main component $^{28}N_2$. However, the use of the signal of $^{29}N_2$ provides more reliable data. The measurements allow to detect different temperature dependent processes, such as the formation of carbon dioxide through oxidation processes, the release of the blowing agents from the sample material, or the degradation of the polymer matrix. The data allows differentiation between different blowing agents for XPS. The temperature range, in which the blowing agents are released from the samples, can be identified, too. The types of blowing agents could be estimated, but further analysis would be required to confirm these findings. HCFC R22 and R142b have been identified as blowing agents used in XPS-B, which are banned from use in many countries. Fig. 10 and Fig. 11 illustrate the condition of the sample materials after the measurement. The samples melted during the heating process and the blowing agent formed bubbles of different sizes. While sample XPS-A retained its original color and shows small bubbles, the samples of XPS-B changed from blue to dark green and black and show large bubbles.

The here described experimental set-up has a mass range of 100 amu limited by the mass spectrometer. In the temperature range in which the measurements were performed volatile molecular species exceeding this mass range have to be considered. Therefore, it can be assumed that the signals of unknown origin originate from fragmentation of heavier ions, which were not detected. A conclusive attribution to specific compounds is not possible on the basis of the existing data. Furthermore, the measurements performed in the presence of oxygen have shown that the identification of oxidation processes is possible. As oxidation processes even occurred with residual oxygen in the test chamber, possible oxidation products have to be considered as sources of low intensity ion signals.

5. Conclusion

5.1. Summary

The described experimental setup provides an easy to use method for measuring outgassing of samples avoiding complicated sample preparation procedures. For the purpose of developing the methodology a material type with a clearly defined temperature range for the release of large amounts of volatile compounds has been selected. With the primary focus on possible material interactions due to the outgassing of volatile compounds under elevated temperatures, the method shows a sufficient sensitivity for the analysis of complex gas mixtures with a broad range of concentrations of individual compounds. This makes is also applicable to polymers with a lower content of volatile compounds and a broad volatilization range. The temperature dependent mass spectra can be visualized as contour plot. It represents the thermal behavior of each sample and provides all relevant mass signals, which require further analysis. In a second step the temperature dependent data for relevant mass signals can be normalized to the mass signal of the inert gas. For data analysis several approaches have been evaluated. The normalization using a combination of the signal intensities of both nitrogen isotopes $^{28}N_2$ and $^{29}N_2$ (Equation (4)) has been identified to be the only one which is not influenced by the possible formation of carbon monoxide with a molecular mass of 28 u.

For the measurements of two different XPS types the signal of the inert gas helium has been used for normalization. Based on the temperature dependency of the intensity the observed signals were attributed mainly to the blowing agents being released at the squatting temperature of the material. The two samples contain different blowing agents of which the agents used in XPS-B were identified as two different HCFCs. Furthermore, both materials show a different resistance against thermal degradation (see Figs. 10 and 11). With a focus on the intended use in polymeric solar thermal collectors a conclusive selection between the two materials can be made. The release of HCFCs from material XPS-B is not only prohibited, but can cause unintended interactions with other materials inside the collector. Consequently, it is not

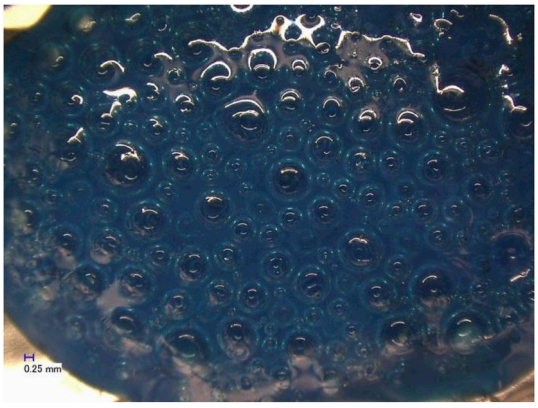

Fig. 10. XPS-A sample after the measurement at up to 250 °C. The sample material has molten and small bubbles have been formed on the surface. The color resembles the sample's initial color.

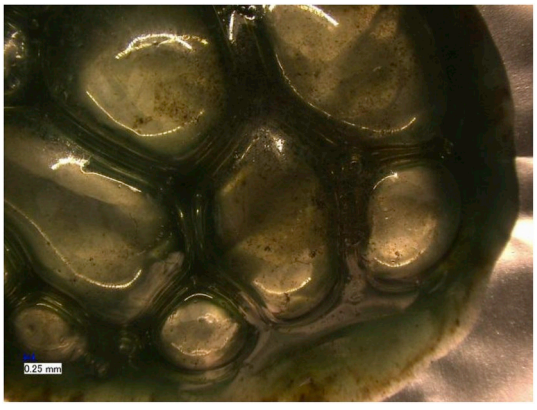

Fig. 11. XPS-B sample after the measurement at up to 250 °C. The sample material has molten and few very large bubbles have been formed in the material. The color has changed to dark green and shows black regions, which indicate a thermal decomposition of the material.

recommended to use this material in such applications.

5.2. Outlook

More information on the involved decomposition products can be obtained by extending the mass range of the mass analyzer. Modifications in the experimental setup can be performed to reduce uncertainties in the time-temperature correlation and to reduce effects of thermal inertia of the setup. At this stage the setup provides a proof of concept and allows exploring possible applications for this kind of outgassing measurements. One possible application could be to test materials for the release of hazardous substance at different temperatures. Comprehensive studies on other base materials for polymeric collectors, like different grades of PPS, have been performed and are subject to successive publications.

Data availability

The raw data required to reproduce these findings cannot be shared at this time due to technical or time limitations. The processed data required to reproduce these findings cannot be shared at this time due to technical or time limitations.

Declaration of competing interest

The authors declare that they have no known competing financial interests or personal relationships that could have appeared to influence the work reported in this paper.

Acknowledgment

This work has been conducted within the EU project SCOOP. The project has received funding from the European Union's Seventh Framework Program for research, technological development and demonstration under grant agreement No: 282638.

Appendix A. Supplementary data

Supplementary data to this article can be found online at https://doi.org/10.1016/j.polymertesting.2019.106164.

References

[1] A. Olivares, J. Rekstad, M. Meir, S. Kahlen, G. Wallner, A test procedure for extruded polymeric solar thermal absorbers, Sol. Energy Mater. Sol. Cells 92 (4) (2008) 445–452.
[2] S. Kahlen, G.M. Wallner, R.W. Lang, M. Meir, J. Rekstad, Aging behavior of polymeric solar absorber materials: aging on the component level, Sol. Energy 84 (3) (2010) 459–465.
[3] S. Kahlen, G.M. Wallner, R.W. Lang, Aging behavior of polymeric solar absorber materials – Part 1: engineering plastics, Sol. Energy 84 (9) (2010) 1567–1576.
[4] S. Kahlen, M. Jerabek, G.M. Wallner, R.W. Lang, Characterization of physical and chemical aging of polymeric solar materials by mechanical testing, Polym. Test. 29 (1) (2010) 72–81.
[5] M. Koehl, S. Saile, A. Piekarczyk, S. Fischer, Task 39 exhibition – assembly of polymeric components for a new generation of solar thermal energy systems, in: Proceedings of the 2nd International Conference on Solar Heating and Cooling for Buildings and Industry (SHC 2013), 48, 2014, pp. 130–136.
[6] M. Köhl, G. Jorgensen, S. Brunold, B. Carlsson, M. Heck, K. Möller, Durability of polymeric glazing materials for solar applications, Polym. Mater. Sol. Energy Appl. 79 (6) (2005) 618–623.
[7] D. Missirlis, G. Martinopoulos, G. Tsilingiridis, K. Yakinthos, N. Kyriakis, Investigation of the heat transfer behaviour of a polymer solar collector for different manifold configurations, Renew. Energy 68 (2014) 715–723.
[8] B. Carlsson, M. Meir, J. Rekstad, D. Preiß, T. Ramschak, Replacing traditional materials with polymeric materials in solar thermosiphon systems – case study on pros and cons based on a total cost accounting approach, Sol. Energy 125 (2016) 294–306.
[9] A.C. Mintsa Do Ango, M. Medale, C. Abid, Optimization of the design of a polymer flat plate solar collector, Sol. Energy 87 (2013) 64–75.
[10] N. Aste, G. Chiesa, F. Verri, Design, development and performance monitoring of a photovoltaic-thermal (PVT) air collector, Renew. Energy 33 (5) (2008) 914–927.
[11] J.-S. Kwon, H. Jung, I.S. Yeo, T.-H. Song, Outgassing characteristics of a polycarbonate core material for vacuum insulation panels, Vacuum 85 (8) (2011) 839–846.
[12] W. Xie, W.-P. Pan, Thermal characterization of materials using evolved gas analysis, J. Therm. Anal. Calorim. 65 (3) (2001) 669–685.
[13] K. Raemakers, J. Bart, Coupling thermal analysis and gas analysis Methods Applications of simultaneous thermogravimetry-mass spectrometry in polymer analysis, Thermochim. Acta 295 (1) (1997) 1–58.
[14] PII: 0040-6031(81)87045-1.
[15] S.M. Dyszel, Thermogravimetry coupled with atmospheric pressure ionization mass spectrometry. A new combined technique, Thermochim. Acta 61 (1–2) (1983) 169–183.
[16] R. Bernstein, S.M. Thornberg, R.A. Assink, A.N. Irwin, J.M. Hochrein, J.R. Brown, D.K. Derzon, S.B. Klamo, R.L. Clough, The origins of volatile oxidation products in the thermal degradation of polypropylene, identified by selective isotopic labeling, Polym. Degrad. Stab. 92 (11) (2007) 2076–2094.
[17] NIST Mass Spec Data Center, S.E. Stein, director (ed) NIST Chemistry WebBook, NIST Standard Reference Database Number 69, Eds. P.J. Linstrom and W.G. Mallard: "(Mass Spectra)".
[18] S.J. P, C.J. B, G. R, D.E. L, Polystyrene/acrylic blends and their application in foam production, in: Part One: R22/142b Blowing Agent, Society of Plastics Engineers, Inc. (SPE), Brookfield Center, CT, 1998.